Adaptive Bit Rate Video Streaming Through an RF/Free Space Optical Laser Link

Ahmet AKBULUT, H. Alparslan ILGIN, Murat EFE

Electronics Engineering Dept., Ankara University, Besevler, 06100 Ankara, Turkey

{aakbulut, ilgin, efe}@eng.ankara.edu.tr

Abstract. *This paper presents a channel-adaptive video streaming scheme which adjusts video bit rate according to channel conditions and transmits video through a hybrid RF/free space optical (FSO) laser communication system. The design criteria of the FSO link for video transmission to 2.9 km distance have been given and adaptive bit rate video streaming according to the varying channel state over this link has been studied. It has been shown that the proposed structure is suitable for uninterrupted transmission of videos over the hybrid wireless network with reduced packet delays and losses even when the received power is decreased due to weather conditions.*

Keywords

Free space laser communication, link availability, adaptive video streaming.

1. Introduction

In the modern communication era, the wireless communication technologies have become a major area of comprehensive research and development. The increasing demand for the channel capacity and bandwidth requirements force the development of advanced wireless systems with high speed and high reliability as well as the flexibility for varying traffic conditions. The objective of future wireless communication systems is to provide users with a wide variety of services such as the internet access, file transfer, interactive data, voice and image transfer comparable to those provided by the wired communication systems. Multimedia traffic may have various service requirements, which result in a larger bandwidth requirement pertaining to the traffic load. Large bandwidth traffic is generally more restricted than small bandwidth traffic load in terms of the availability of the system resources. Therefore the system capacity is mainly determined by the large bandwidth traffic and, despite its disadvantages in adverse weather conditions, optical wireless communication is a good alternative for improving the bandwidth and system capacity.

With the recent developments in the semiconductor technology, FSO communication, or optical wireless has become an attractive alternative to optical fiber links, as well as to radio frequency (RF) systems. FSO systems offer much higher data rates compared to RF systems and also easier to install and much less expensive than the underground fiber. Although, fiber-optic communication is still the preferred media for long distances, FSO is now considered as a judicious option to fiber for the short distances of 4 km or less [1-5].

However, despite the advantages that an FSO system holds, there is one big challenge for optical wireless, that is the atmospheric attenuation of the transmitted laser beam [6-8]. The attenuation is caused as a result of various factors which can be listed as follows:

- *absorption* (appears primarily because of the water vapor and carbon dioxide),
- *scattering* (related to the wavelength used and the number and size of scattering elements in the atmosphere such as fog),
- *shimmer* (arises from the combination of atmospheric turbulence, air density, light refraction, cloud cover and wind).

The combined effect of all these factors appears as the atmospheric attenuation coefficient in the link budget equation that yields the level of received power at the receiver and is uncontrollable in an outdoor environment. On the other hand, not surprisingly, in heavy attenuation conditions the operation of an FSO link cannot be always maintained, which reduces the availability. This problem should be addressed properly in order to achieve a high available link. A practical solution to this problem would be to back up the FSO link with a lower data rate RF link. In fact, having a radio and laser in tandem works particularly well since microwave transmission is affected more by rain as the carrier wavelength is closer to the size of rain drops whereas the laser transmission is more affected by fog. Hence, the only weather condition that could affect the transmission of a hybrid FSO/RF system is the condition of simultaneous heavy rain and thick fog. Qualitatively, it could be said that these conditions would not occur simultaneously, because as the rain falls the rain droplets would absorb the suspended fog water droplets, thus diminishing the fog.

Although the switching between FSO and RF links according to the varying atmospheric conditions will affect

data rates and the received power, such a setup would provide a high available wireless link for data transmission that will be active in almost any weather condition. Any reduction in the received power would result in information losses and delays. For instance if video streaming at a constant bit rate is attempted in the existence of received power reduction, then it will cause picture freeze, frame jumps and restarting of the video at the receiver. On the other hand such problems would be properly addressed by simply monitoring the channel state and lowering the bit rate to a rate that would help maintain a certain level of video quality. In this study, an adaptive bit rate video streaming structure is proposed based on the atmospheric data collected over the months of January, February, March and April when the most adverse weather conditions appear for free space optical communication.

The high available communication link has been set up for video conferencing and remote lecturing between the two campuses of Ankara University. Ankara University is one of the biggest universities in Turkey and has five campuses each encompassing several faculties that are situated at different locations around the city. In order to increase the availability of the link, an RF back-up link has been decided to be integrated with the FSO system.

2. System Definition

The FSO/RF link has been designed to make use of the best features of two transport mediums, laser light and radio waves to form a single, high available and seamless wireless communication link between the two campuses. As shown in Fig. 1, the system comprises four sub-systems, namely, 1) adaptive video encoder, 2) laser link, 3) switch, and 4) RF link.

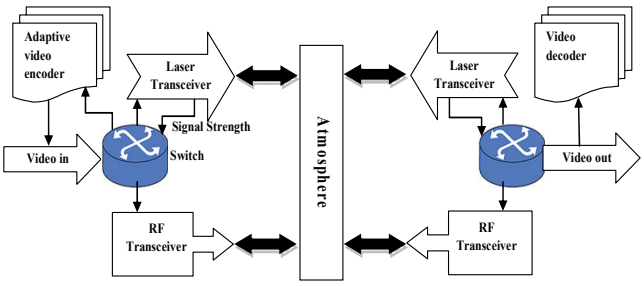

Fig. 1. Schematic diagram of the adaptive video streaming scheme over the FSO/RF hybrid link.

The laser link refers to a pair of FSO transceivers each aiming a laser beam at the other, creating a full duplex communication link. A laser system requires careful planning and analysis prior to equipment installation. A poorly designed path may result in periods of system outages, increased system latency, decreased throughput or a complete failure of communication across the link. Hence, before determining the link feasibility, link's atmospheric attenuation and geometrical spreading loss must be calculated.

Despite the availability of high power, in heavy attenuation the laser signal might still get degraded. Therefore, the signal level at the receiver is checked every 5 seconds and when the received signal level falls below a certain threshold, the laser stops transmitting data to the switch. As soon as the degradation at the signal level is detected, the system automatically switches over to the RF link, which is waiting as a hot stand-by. Thus, despite the reduction in the bandwidth, the link remains available. The RF link is a very good complement to FSO as an RF link has very little problem penetrating fog, which poses a big problem for FSO [9-13]. FSO on the other hand has little problem with rain, microwave radio's biggest adversary. Thus, an FSO/RF hybrid system provides almost an all-weather communication link.

The RF part of the system has been chosen to operate at 2400 MHz-2483.5 MHz (13 channels) ISM frequency band and use 802.11b DSSS technology. After the switchover to the RF link it stays as the primary link until the received signal level goes over a higher threshold, indicating that a solid connection on the laser link can be re-established. When the increased signal level is detected, the system switches back to the laser link. The threshold level on the received laser power must carefully be determined for a seamless switchover to the RF link. In threshold level calculations, losses of optical components have been neglected and a 3 dB margin has been added on top of the calculated level in order to account for then neglected optical component losses. Even when the system switches to the radio, the received power level is still monitored for a quick recovery of the laser link so that a much higher bandwidth could be utilized. However, the system does not switch back over to the laser link even when the FSO-to-RF switchover threshold power level is achieved again. In fact, the power level to go back on the FSO is higher than the FSO-to-RF threshold. The reason for having two different switchover thresholds (a higher one for switching back to the laser from the radio than the one to switch from the laser to the radio) is to reduce the switchover frequency and prevent the system switching back and forth constantly.

2.1 Channel Model

The channel is the atmosphere in wireless communication. Laser links can be affected by a variety of atmospheric phenomena, fog and scintillation being the most common by far. Free space, low altitude laser transmissions are range and bit error limited by the atmospheric energy losses resulting from scattering during haze, rain, snow, and fog conditions in the atmospheric channel. Most free space laser transmission wavelengths are primarily chosen for their very low absorption losses, so that molecular energy transitions do not absorb free space laser energy.

The attenuation of laser power through the atmosphere is described by the exponential Beers-Lambert Law [14].

$$\tau(R) = \frac{P(R)}{P(S)} = e^{-\sigma R} \tag{1}$$

where $\tau(R)$ is the transmittance at range R, $P(R)$ is the laser power at range R, $P(S)$ is the laser power at the source, and σ is the attenuation or total extinction coefficient per unit length.

The attenuation coefficient has contributions from the absorption and scattering of laser energy by different aerosols and molecules in the atmosphere. Since the laser wavelength is chosen to fall inside transmission windows of the atmospheric absorption spectra, the contributions of absorption to the total attenuation coefficient are very small. The effects of scattering, therefore, dominate the total attenuation coefficient. The type of scattering is determined by the size of the particular atmospheric particle with respect to the transmission laser wavelength.

The final atmospheric phenomenon that significantly impacts laser propagation is scintillation. At low altitudes, scintillation effects arise from the temperature differences between the ground and air and the resulting heat exchange. The index of refraction of air changes with temperature and the heat exchange causes local index variations that have different scale sizes that effect the laser propagation [15]. The index changes result in lensing effects along the optical path. The dominant scintillation effect occurs when the scintillation scale is comparable to the beam size. This scale size event defocuses the beam and leads to significant intensity variations in the received amplitude of the laser signal. To overcome these coherent events, systems have used multiple transmitting apertures of sufficient separation and temporally incoherent laser transmissions. As a result, the systems have regained some of the fade losses by making the individual beams uncorrelated to the atmospheric scale size.

To determine the atmospheric attenuation of optical signals, the equation is utilized to base the attenuation on the visibility and the incident wavelength λ [16].

$$\sigma = \frac{3.91}{V}\left(\frac{\lambda}{550nm}\right)^{-\delta} \tag{2}$$

where, σ is the atmospheric attenuation (or scattering) coefficient, V is the visibility (in km), λ is the wavelength (in nm) and δ is the size distribution of the scattering particles. δ = 1.6 indicates a good visibility (V > 50 km), where as δ = 1.3 indicates a moderate visibility. Tab. 1 presents the atmospheric attenuation values at 1550 nm band calculated using (2).

Visibility (km)	0.1	0.2	0.3	0.5	1	2	3	5	10	20	50
A_{Atm}, dB/km 1150 nm	128.2	59.6	37.7	20.9	9.2	3.9	2.3	1.2	0.44	0.22	0.06
Weather	Fog					Haze			Clear		

Tab. 1. Atmospheric loss (in dB/km) with respect to visibility at 1550 nm.

A mathematical model for optical signals and noise is derived and SNR of the proposed laser communication system is determined. The link budget can be defined in standard RF communication terminology. The received power at the detector is given as follows.

$$P_R = P_T\left(\frac{\lambda}{4\pi R}\right)^2 G_T G_R A_{Atm} \tag{3}$$

where P_R is the received power, P_T is the transmitted power, A_{Atm} is the atmospheric attenuation factor, and R is the distance between the communicating stations. The term in the brackets is the free space loss and G_T and G_R are the transmitter and receiver telescope gains respectively given by

$$G_T \approx \left(\frac{\pi D_T}{\lambda}\right)^2, \tag{4}$$

$$G_R \approx \left(\frac{\pi D_R}{\lambda}\right)^2 \tag{5}$$

where D_T and D_R are the transmitter and receiver aperture diameters respectively.

For optical detection using photo detectors, the SNR can be written as [17]

$$SNR = \frac{(P_s R_d)^2}{N_0 B} \tag{6}$$

where P_s is the required peak signal in watts, R_d is the responsivity of the detector in amps per watt, N_0 is the noise density in amps squared per hertz, and B is the receiver bandwidth in hertz.

The noise in OOK direct-detection systems can be modeled as the quadrature sum of all the noise densities and is given by

$$N_0 B = i_d^2 + i_t^2 + i_{ss}^2 \tag{7}$$

where i_d^2 is the detector dark noise, i_t^2 is the thermal noise and i_{SS}^2 is the signal shot noise. The noise sources are expressed mathematically by

$$i_d^2 = 2qBI_d, \tag{8}$$

$$i_{ss}^2 = 2qI_s B, \tag{9}$$

$$i_t^2 = \frac{4kTB}{R} \tag{10}$$

where I_d is the average dark current, B is the photodiode bandwidth, q is the electron charge, k is the Boltzmann's constant, T is the absolute temperature (^{o}K), and R is the photodiode load resistor.

Now the signal to noise ratio can be expressed in terms of total signal power and total noise power.

$$SNR = \frac{(P_s R_d)^2}{N_0 B} = \frac{I_s^2}{i_t^2 + i_d^2 + i_{ss}^2}. \tag{11}$$

The parameters taken into account when calculating the link equation of the transmitter and receiver used in the laser subsystem are given in Tab. 2.

Link distance	2.9 km
Laser output power	640 mW (4 transmitter at 160 mW)
Wavelength	1550 nm
Transmitter type	Directly modulated laser diode
Modulation scheme	OOK (NRZ waveform)
D_T, D_R	5 cm, 20 cm
Detector responsivity (PIN)	0.9 A/W
Detector dark current	0.3 nA (max)

Tab. 2. Transmitter and receiver parameters of the laser system.

2.2 Laser Power Requirement and Channel Statistics

Given the SNR, then the required power at the receiver to produce a desired BER value can then be calculated for OOK modulation. Also, how much power must be transmitted under different noise and atmospheric attenuation conditions, can be derived from the required power. The responsivity of the PIN detector employed in the system is 0.9 A/W, which has the dark current level of 0.3 nA (max) and for BER = 10^{-9} the required power to achieve this probability is calculated as *P*req = 3.5 μW. With a 3 dB link margin, the required power becomes *P*req = 7 μW for a good quality transmission through laser. Therefore, 7 μW has been chosen as the threshold on received laser power level to switch to the radio. Every time the received power goes below the 7 μW threshold a switchover occurs and the RF link becomes operational. The power level to be reached again in order to resume transmission through laser again has set at 10 μW for the reasons defined above.

Fig. 2 depicts the calculated received power level with range (up to the communication range) at different visibility values. The first horizontal line from bottom indicates the calculated 3.5 μW power level. The next horizontal line up from it is the threshold power level, that is 7 μW, thus, the region below that threshold level can be considered as the RF region, i.e., the region where the radio is active.

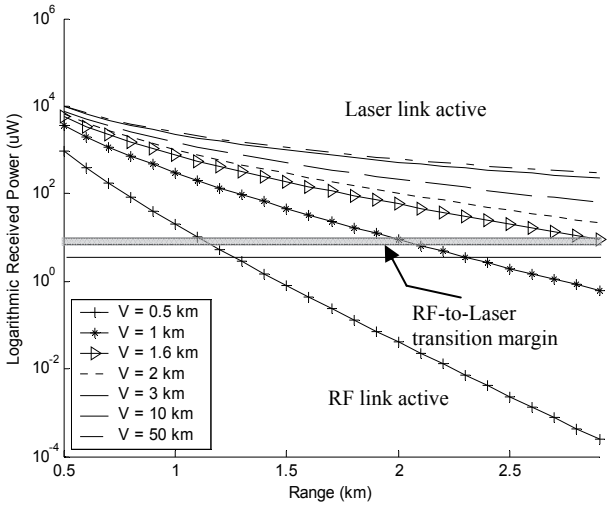

Fig. 2. Received power vs. range for different visibility levels.

The top line in Fig. 2 is the RF-to-FSO switchover threshold (10 μW) and the region above the threshold line shows the region and visibility levels where the FSO is active. As can be seen from Fig. 2, for a switchover from radio to laser, the visibility must increase to 1.6 km for the experimental system.

The experimental RF/Laser link may be disturbed by external objects such as flying birds. These interruptions and fluctuations on the received power increase bit errors and latency, especially when TCP protocol is used for communication. As a consequence total link throughput will decrease. In our scheme, these negative effects can be prevented with the usage of different bit rate source coding in both RF and laser link. When the weather conditions get better, the proposed video encoder can transmit at higher bit rates.

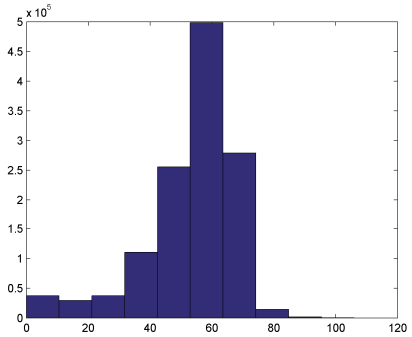

Fig. 3. Histogram of the received power (μW) over 4 months.

Fig. 3 displays the histogram of the power values collected at every 5 sec at the receiver. A total of 1,262,748 data have been utilized for generating the power statistics. Distribution of the power values are tabulated in Tab. 2.

Received power intervals (μW)	Distribution (%)
0-5.3	2.9573
15.9	2.3258
26.5	2.9242
37.1	8.7280
47.7	20.2251
58.3	39.4804
68.9	22.0890
79.5	1.1423
90.1	0.1182
100.7-106	0.0097

Tab. 3. % distribution of the received power in 10 μW intervals for 4 months.

As it can be seen from Tab. 3, over 80% of the time the received power is above 47.7 μW during adverse weather conditions. These received power statistics will later be employed in determining the various bit rate levels for adaptive bit rate video coding.

3. Video Encoder

Designing adaptive video streaming applications over TCP/UDP-IP network infrastructure based on the network

traffic, channel state, packet losses and delays have been the focus of attention in recent years [18-25]. Various methods, for evaluating the quality of the video transmitted over packet networks are available [26], [27]. In this study a zerotree coding based video encoder has been used for video coding and Peak Signal to Noise Ratio (PSNR), an objective quality measure, has been utilized for quality assessment. Although adaptive bit rate video streaming over TCP/UDP-IP network is commonly encountered, the use of the adaptive bit rate technique over an FSO laser/RF hybrid link has been newly studied. The zerotree coding based video encoder has been designed to employ different bit rates that have been selected based on the observed FSO channel statistics. Using Tab. 3, power ranges for the four different bit rates have been selected as 7 μW to 26.5 μW, 26.5 μW - 37.1 μW, 37.1 μW - 47.7 μW and > 47.7 μW. The four different bit rates for the given power ranges are 64, 128, 256 and 512 kbps respectively. When the RF link is active the coding is done at the lowest bit rate employed by the encoder. However, video coding scheme does not necessarily perform at the given exact bit rates. Bit rates are adjusted instantly according to the power fluctuations. Within this concept, coding has been carried out even at the bit rates less than 64 and greater than 512 kbps regarding to the power level.

Video coding system has mainly four parts, which are full search motion estimation and compensation for inter-frame coding, Discrete Cosine Transform (DCT), quantization and entropy coding as shown in Fig. 4.

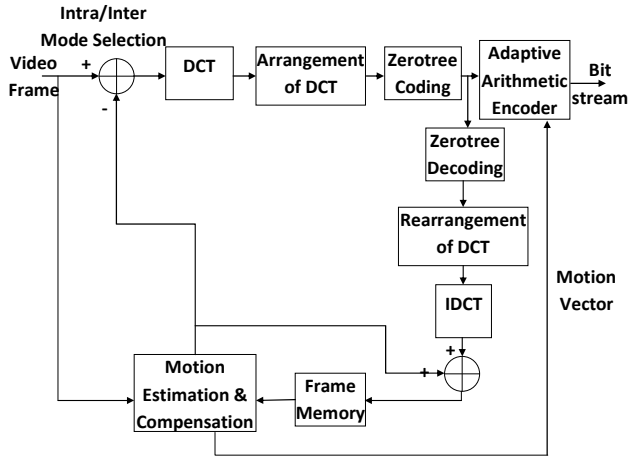

Fig. 4. Video encoder with zerotree coding.

To compress video efficiently and perform bit rate control, regular quantization scheme, which uses quantization parameter and is used in most common video coding standards such as H.263 and H.264, was replaced with zerotree coding [28]. Zerotree coding is performed efficiently as it was implemented in [29] which is called Set Partitioning in Hierarchical Trees (SPIHT). Subsequently, adaptive arithmetic coder is used to encode symbols obtained by the zerotree coding since it outperforms Huffman coding, one of the most common entropy coding methods used in image and video coding standards, in terms of compression ratio [28], [29], [30]. In order to perform zerotree coding, block structured 8x8 DCT coefficients are reformed into subbands [30]. We rearranged DCTs into seven subbands. At each subband, there exists a dependency as a tree structure between the coefficients at the same orientation. A zerotree can be encoded by a single symbol if all the branches of the tree are below a certain threshold for current iteration resulting in efficient coding [28], [29]. By the use of zerotree coding, DC values, which have most of the energy of the related block, are initially encoded. Then AC coefficients are encoded in decreasing order [31]. A detailed explanation of SPIHT can be found in [29]. At 512 kbps we obtain 40.76 dB average PSNR with SPIHT type zerotree coding while regular quantization case gives 38.06 dB.

Frame dropping is almost prevented with the transmission of importance-ordered DCT coefficients. For instance if channel condition gets worse, encoding of a frame can be ceased instantly. At the decoder side, coefficients, received until that moment, are decoded. Related frame can be reconstructed only using those coefficients. Accordingly the frame is avoided from dropping. Decoder can also adjust itself related to its buffer level. At any decoding time, if channel condition gets better, encoder bit rate increases filling the buffer of the decoder. If buffer occupancy gets too high then decoder can stop decoding the current frame to decode the next one. Fort both cases, reconstructed frames are visibly reasonable since some or all of the DC coefficients even with some ACs are already decoded. This flexibility also provides the video coding system to adapt its bit rate to the changing channel conditions. In regular quantization case, all DCT blocks should be decoded to reconstruct the whole frame.

At very low bit rates, since most of the AC coefficients are coded as zero, quality of the reconstructed frames decreases. By the use of the decimation, less important high frequency AC coefficients are ignored giving priority to lower frequency AC coefficients. We used frame size decimation in the DCT domain for several decimation factors in conjunction with zerotree coding to obtain efficient coding at very low bit rates when necessary [30]. At the decoder, interpolation is applied to obtain the decoded frames at full size. Both decimation and interpolation are performed at the DCT domain more efficiently than the ones in the spatial domain [30]. Decimation/interpolation scheme is effective especially at 64 kbps and lesser bit rates. When decimation by 2 is used, corresponding interpolation by 2 is performed at the receiver in order to obtain video frames at the original size. Also decimation after DCT and interpolation after rearrangement of DCT are added to the video encoder shown in Fig. 4. We coded CIF (288x352 pixels) videos at 30 frames/s at several bit rates. In the second and third columns of Tab. 4, average PSNR results of the decoded frames which are encoded with SPIHT type zerotree coding with full size frame video coder and quarter size frame video coder are shown respectively. As seen from Tab. 4, there is no need to use decimation when encoding video at high bit rates such as 128, 256 and 512 kbps.

Bit Rate (kbps)	Full size coding (dB)	Coding with decimation by 2 (dB)
512	40.76	38.81
256	39.82	38.50
128	38.80	38.11
64	37.92	37.49

Tab. 4. Average PSNR values of decoded video frames.

However as the weather condition gets worse and the bit rate decreases, coding with decimating video frames by 2 gives better results. When coding with 64 kbps, average PSNR of the decoded video frames encoded with decimation by 2 is almost the same with the one of the full size coding as shown in Tab. 4. We also run the simulations at lower bit rates to test the effectiveness of the decimation. For instance, average PSNR values at 16 kbps for full size coding and coding with decimation by 2 are 35.00 dB and 36.08 dB respectively.

4. Conclusion

In this paper design criteria on an FSO link for video transmission to 2.9 km distance have been given and adaptive bit rate video streaming according to the varying channel state over this link has been studied. The laser link is equipped with a back up RF link for uninterrupted transmission in all weathers. The video encoder has been designed to code at different bit rate levels to be utilized at varying received power levels. The bit rate levels to be used in the adaptive structure have been determined based on the received power data collected over the months that display the most adverse weather conditions. The resulting structure is suitable for uninterrupted transmission of videos over the FSO network with reduced packet delays and losses even when the received power is decreased due to weather conditions. Channel statistics reveal that over 80% of the time the received signal level is greater than 47.7 μW indicating that the channel allows video streaming at the best rate possible for most of the time. Besides, there exist some rapid fluctuations of the power of laser signal at small time periods in some seasons as seen in Fig. 5.

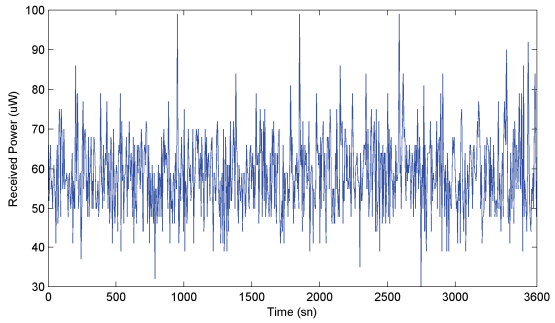

Fig. 5. Received power (μW) in February for 1 hour.

Consequently bit rates are instantly adjusted to the power fluctuations. By frame decimation performed in the DCT domain, coding has been handled at higher quality levels when compared to full size coding at low bit rates such as 64 kbps and less. When decimation is used, frames are interpolated to their original size at the receiver.

References

[1] CARBONNEAU, T. H., WISELY D. R. Opportunities and challenges for optical wireless; the competitive advantage of free space telecommunication links in today's crowded marketplace. In *SPIE Conference on Optical Wireless Communications.* Massachusetts, 1998, p. 119-128.

[2] WISELY, D. R., McCULLAGH, M. J., EARDLEY, P. L., SMYTH, P. P., LUTHRA, D., DE MIRANDA, E. C., COLE, R. S. 4-km terrestrial line-of-sight optical free-space link operating at 155 Mbit/s. *Free Space Laser Communication Technologies VI*, *Proceedings of SPIE*, vol. 2123, 1994, p. 108-119.

[3] AKBULUT, A., EFE, M., CEYLAN, A. M., ARI, F., TELATAR, Z., ILK, H. G. An experimental hybrid FSO/RF communication system. In *Proceedings of the IASTED International Conference on Communication System and Networks*, CSN 2003, p. 406-411.

[4] SMOLYANINOV, I., WASICZKO, L., CHO, K., DAVIS, C. Long-distance 1.2 Gb/s optical wireless communication link at 1550 nm. *Free-Space Laser Communication and Laser Imaging, Proceedings of SPIE*, vol. 4489, 2002, p. 241-250.

[5] YIN, F. Optical interconnects for telecommunication and data communications. *Optical Interconnects for Telecommunication and Data Communications, Proceedings of SPIE,* vol. 4225, 2000, p. 223-227.

[6] TAN, Y., GUO, JIAN-ZHONG. Study of channel model of free-space laser communications system. *Free-Space Laser Communications V, Proceedings of SPIE,* vol. 5892, 2005, pp.223 to 227.

[7] MAJUMDAR, A. K., RICKLIN, J. C. Effects of the atmospheric channel on free-space laser communications. *Free-Space Laser Communications V, Proceedings of SPIE,* 2005, vol. 5892, p. 58920K.1-58920K.

[8] MANOR, H., ARNON, S. Performance of an optical wireless communication system as a function of wavelength. *Applied Optics*, vol. 42 (21), 2003, p. 4285-4294.

[9] NADEEM, F., LEITGEB, E., SALEEM AWAN, M., KANDUS, G. FSO/RF hybrid network availability analysis under different weather conditions. In *Third International Conference on Next Generation Mobile Applications, Services and Technologies*, IEEE Computer Society Press, p. 239-244, 2009.

[10] ZHANG, W., HRANILOVIC, S., CE SHI. Soft-switching hybrid FSO/RF links using short-length raptor codes: Design and implementation. *IEEE Journal on Selected Areas in Communications,* vol. 27, no. 9, p. 1-11, December 2009.

[11] NADEEM, F., LEITGEB, E., AWAN, M. S., KHAN, M. S., KANDUS, G. Throughput efficient solution for hybrid wireless network. In *IEEE International Workshop on Satellite and Space Communications*, 2008. IWSSC 2008., p. 316-320, 2008.

[12] KIM, I., KOREVAAR, E. J. Availability of free-space optics (FSO) and hybrid FSO/RF systems. In *Proceedings Optical Wireless Communications IV*, vol. 4530, Eric J. Korevaar, Editors, p. 84-95, 2001.

[13] TZUNG-HSIEN, H., SUGIANTO, T., ANIKET, D., JAIME, L., STUART, D. M., CHRISTOPHER, C. D. Performance and analysis of reconfigurable hybrid FSO/RF wireless networks. In *Proceedings Vol. 5712, Free-Space Laser Communication Technologies XVII*, G. Stephen Mecherle, Editors, p. 119-130, 18 April 2005.

[14] KIM, I., McARTHUR, B., KOREVAAR, E. J. Comparison of laser beam propagation at 785 nm and 1550 nm in fog and haze for optical wireless communications. *Optical Wireless Communications III, Proc. SPIE*, vol. 4214 (26), 2001, p. 26-37.

[15] KARP, S., GAGLIARDI, R. M., MORAN, S. E., STOTTS, L. B. *Optical Channels*. New York: Plenum Press, 1988.

[16] KIM, I., McARTHUR, B., KOREVAAR, E. J. Comparison of laser beam propagation at 785 nm and 1550 nm in fog and haze for optical wireless communications. In *SPIE Photonics East/Optical Wireless Communications III*, 2000, p. 26 - 37.

[17] LAMBERT, S. G., CASEY, W. L. *Laser Communications in Space*. Boston: Artech House, 1995.

[18] DAPENG WU HOU, Y. T., YA-QIN ZHANG Scalable video coding and transport over broadband wireless networks. *Proceedings of the IEEE*, vol. 89 (1), p. 6-20, 2001.

[19] LEE, S., CHUNG, K. Joint quality and rate adaptation scheme for wireless video streaming. In *22nd International Conference on Advanced Information Networking and Applications*, 2008, p. 311 to 318.

[20] RAMANUJAN, R. S., NEWHOUSE, J. A., KADDOURA, M. N., AHAMAD, A., CHARTIER, E. R., THURBER, K. J. Adaptive streaming of MPEG video over IP networks. In *22nd Annual IEEE International Conference on Local Computer Networks* (LCN'97). Minneapolis (MN), 1997, p. 398-409.

[21] AL-SUHAIL, G., WAKAMIYA, N., FYATH, R. S. Error-resilience of TCP-friendly video transmission over wireless channel. In *Ninth International Conference on Control, Automation, Robotics and Vision*, 2006, p. 1-6.

[22] YASER, P. F., HASSAN, M., SALMAN, K., PANOS, N., HUSSEIN, M. A. A link adaptation scheme for efficient transmission of H.264 scalable video over multirate WLANs. *IEEE Transactions on Circuits and Systems for Video Technology*, vol. 18 (7), 2008, p. 875 - 887.

[23] BERND, G., MARK, K., YI J. LIANG, RUI ZHANG Advances in channel-adaptive video streaming. *Wireless Communications and Mobile Computing*. 2002, p. 573–584.

[24] HUIFANG SUN, ANTHONY, V., JUN XIN An overview of scalable video streaming. *Wireless Communications and Mobile Computing*. 2007, p. 159–172.

[25] PASQUALINI, S., FIORETTI, F., ANDREOLI, A., PIERLEONI, P. Comparison of H.264/AVC, H.264 with AIF, and AVS based on different video quality metrics. In International Conference on Telecommunications, 2009. ICT '09, 2009, p. 190-195.

[26] LIUMING LU, XIAOYUAN LU Quality assessing of video over a packet network. In *Second Workshop on Digital Media and its Application in Museum & Heritage* (DMAMH 2007), 2007, p. 365-369.

[27] KWANGJIN CHOI, JUN KYUN CHOI, JAE HWAN HONG, GYEONG JU MIN, JONGKUK LEE Comparison of video streaming quality measurement methodologies. In *10th International Conference on Advanced Communication Technology*, 2008. ICACT 2008, 2008, p. 993-996.

[28] SHAPIRO, J. M. Embedded image coding using zerotrees of wavelet coefficients. *IEEE Trans. Signal Process*., vol. 41, no. 12, Dec. 1993, p. 3445–3462.

[29] SAID, A., PEARLMAN, W. A. A new, fast, and efficient image codec based on set partitioning in hierarchical trees. *IEEE Trans. Circuits and Syst. for Video Technology*, 1996, vol. 6, no. 3, p. 243-250.

[30] ILGIN, H. A., CHAPARRO, L. F. Low-bit rate video coding using DCT-based fast decimation/interpolation and embedded zerotree coding. *IEEE Trans. Circuits and Syst. for Video Technology,* 2007, vol. 17, no. 7, p. 833-844.

[31] XIONG, Z., GULERYUZ, O. G., ORCHARD, M. T. A DCT-based embedded image coder. *IEEE Signal Process. Lett.*, vol. 3, no. 6, Nov. 1996, p. 289–290.

About Authors

Ahmet AKBULUT received his B.S. degree in Electronics Engineering from the Ankara University in 1998. He received his M.S. and Ph.D. degrees in Electronics Engineering from the same university in 2000 and 2006, respectively. He is a Research Assistant with the Electronics Engineering Department, Ankara University. His research interests include digital communication, optical communication and mobile robotics.

Hakki Alparslan ILGIN was born in Kayseri, Turkey. He received the B.S. and M.S. degrees in Electronics Engineering from Ankara University, Ankara, Turkey in 1993 and 1997, respectively, and the Ph.D degree in Electrical and Computer engineering from University of Pittsburgh, Pittsburgh, PA, USA in 2004. He worked for two years as a Research Assistant and one year as a Teaching Assistant for University of Pittsburgh. He is currently with the Electronics Engineering Department, Ankara University. He is interested in statistical signal processing, image and video coding.

Murat EFE received his B.Sc. and M.Sc. degrees in Electronics Engineering from Ankara University, Turkey in 1993 and 1994 respectively. He received his Ph.D. degree from the University of Sussex, UK in 1998. He worked as a post doctoral fellow at Ecole Polytechnique Fédérale de Lausanne in Switzerland following his Ph.D. degree. He has been with the Electronics Engineering Department at Ankara University since 2000 where he both teaches and conducts research. His research interests include Kalman filtering, multi-target multi-sensor tracking, detection and estimation, cognitive radar, passive network sensing, optical beam tracking.